Capillary Force-Driven, Hierarchical Co-Assembly of Dandelion-Like Peptide Microstructures

Yuefei Wang, Renliang Huang, Wei Qi, Yanyan Xie, Mengfan Wang, Rongxin Su, and Zhimin He*

The wetting and drying of drops on flexible fibers occurs ubiquitously in nature, and the capillary force underlying this phenomenon has motivated our great interest in learning how to direct supramolecular self-assembly. Here, the hierarchical co-assembly of two aromatic peptides, diphenylalanine (FF) and ferrocene-diphenylalanine (Fc-FF), is reported via sequential, combinatorial assembly. The resulting dandelion-like microstructures have highly complex architectures, where FF microtube arrays serve as the scapes and the Fc-FF nanofibers serve as the flower heads. Homogeneous FF microtubes with diameters tailored between 1 and 9 μm and wall thickness ranging from 70 to 950 nm are initially formed by controlling the degree of supersaturation of the FF and the water content. Once the FF microtubes are formed, the growth of the dandelion-like microstructures is then driven by the capillary force, derived from the wetting and drying of the Fc-FF solution on the FF microtubes. This simple and ingenious strategy offers many opportunities to develop new and creative methods for controlling the hierarchical self-assembly of peptides and thus building highly complex nano and microstructures.

Dr. Y. Wang, Prof. W. Qi, Dr. Y. Xie, Dr. M. Wang, Prof. R. Su, Prof. Z. He
State Key Laboratory of Chemical Engineering
School of Chemical Engineering and Technology
Tianjin University
Tianjin 300072, P.R. China
E-mail: qiwei@tju.edu.cn

Dr. R. Huang
School of Environmental Science and Engineering
Tianjin University
Tianjin 300072, P.R. China

Prof. W. Qi, Prof. R. Su
Collaborative Innovation Center of Chemical Science and Engineering (Tianjin)
Tianjin 300072, P.R. China

Prof. W. Qi, Prof. R. Su
Tianjin Key Laboratory of Membrane Science and Desalination Technology
Tianjin University
Tianjin 300072, P.R. China

DOI: 10.1002/smll.201403645

1. Introduction

The hierarchical self-assembly of complex micro or nanostructures from simple building blocks is of fundamental interest to researchers in the nanoscience field. The ability to program the formation of such structures is crucial to enabling their use in technological applications.[1–3] One promising research direction involves the use of such methods to create self-assemblies of short peptides. This direction has been an active area of research over the past few decades, and a wide variety of peptide nanostructures, such as nano or microtubes, nanofibers, nanohelices, nanovesicles, and nanoarrays, have been generated.[4–12] In biological systems, highly functional and complex structures are built via the co-assembly of multiple components under dynamic conditions (e.g., enzyme-substrate recognition and biomineralization).[13] Inspired by these phenomena, several peptide-based, co-assembly systems have been developed to produce functional materials with hierarchical architectures, such as biomolecular necklaces and multi-functional porous microspheres.[14–18] However, most of the strategies reported to control hierarchical

self-assembly processes are still focused primarily on defining the initial conditions. On the contrary, the emergence of complex architectures is attributed to changes in conditions during growth in natural or biological systems.[1,19] We typically have little control over this process, despite the fact that we can choose the starting conditions; thus, it is difficult for us to control the interactions between components and precisely tailor the resulting complex architectures during hierarchically self-assembly processes. As a result, it is compelling for us to design novel peptide co-assembling systems through rationally programmed modulations of the reaction conditions during the hierarchical assembly process. Such control may allow for the formation of highly functional and complex peptide micro or nanostructures.

Wetting–drying phenomena abound in nature (e.g., the "coffee ring" effect,[20] tears of wine,[21] wetting of fibers.[22–24] The capillary forces underlying these phenomena could be used to control hierarchical self-assembly processes. For instance, using the "coffee ring" effect as inspiration, Lin and co-workers rationally designed a series of geometric modules to precisely control the self-assembly of nanoparticles, polymers, or DNA strands into periodic patterns on surfaces.[25–29] Wetting–drying effects were also utilized with carbon nanotube arrays and polymeric nanobristles to form diverse, complex patterns via the forming or twisting of fibers driven by elastocapillary forces.[30–32] However, the translation of these physical regimes to the process of molecular co-assembly, in which hierarchical, complex micro or nanostructures are formed, has not yet been reported. Our group is devoted to the study of the self-assembly of short aromatic peptides, including diphenylalanine (FF)[12,33,34] and designed ferrocene-diphenylalanine (Fc-FF).[8] Previously, it has been demonstrated that FF could self-assemble into nano or microtubes and nanowires as well as vertically aligned arrays and be used in applications involving templatation,[4,35,36] drug release,[37] the formation of superhydrophobic surfaces,[38] biosensing,[39] piezoelectric devices,[40,41] and optics.[42,43] Fc-FF has a redox-active ferrocene moiety at its *N*-terminal, and it can self-assemble into nanospheres and nanofibers under kinetic control.[8] The research community is interested in being able to control the co-assembly of these short functional peptides, and it has shown great interest in the preparation of highly complex structures.

In this work, we report the capillary force-driven, hierarchical co-assembly of FF and Fc-FF moieties into dandelion-like peptide microstructures; this process is achieved via the rational design and stepwise assembly of the structures. We changed the reaction conditions at different stages of the hierarchical self-assembly process by modulating particular experimental parameters, such as the degree of supersaturation, water content, and the nature of the solvent evaporation, to construct intricate, predefined peptide microstructures. FF microtubes with tunable diameters and wall thickness were initially achieved, which provided the essential geometry to induce capillary forces during the evaporation of the solvent. Because the Fc-FF peptides showed different assembly behavior from that of the FF peptides at the different water contents that were examined, the subsequent wetting and drying of the liquid drops containing Fc-FF molecules on the FF microtube arrays triggered the growth of the Fc-FF nanofibers at the cross-points of the FF microtubes. This hierarchical co-assembly behavior finally led to the formation of novel dandelion-like peptide microstructures, where the FF microtubes served as the "scapes" and the Fc-FF nanofibers served as the "flowers." The co-assembled FF/Fc-FF microflowers, which are considered a type of biocompatible peptide material, may have great potential for use as components in biosensing schemes, optical devices, and superhydrophobic surfaces.

2. Results

2.1. Wetting and Drying of Fc-FF Solution on Two Parallel Glass Fibers

Recently, Stone and co-workers undertook a comprehensive investigation of the wetting and drying of liquid drops on flexible fibers, a common physical process in both natural and industrial applications.[22–24] To simplify the physical model, they used drops of silicone oil, a perfectly wetting liquid that does not contain any solutes. However, the wetting and drying phenomena for drops of solutions containing self-assembling peptides are not well understood. Thus, we investigated the wetting and drying of a solution (20% H_2O/80% HFIP, v/v) containing Fc-FF (5 mg mL^{-1}) on two parallel flexible glass fibers (50 μm in diameter, 2.6 cm in length). **Figure 1**a shows a typical wetting and drying scenario achieved by depositing 1 μL of a Fc-FF peptide solution on a pair of parallel fibers (150 μm apart) that are clamped at one end and free to move at the other end. When drops were placed on the fiber arrays close to the clamped ends, the fibers deflected inwards, and the drops moved toward the free ends as a result of capillary forces. Then, the drops at the free ends adopted a compact shape because of the balance between fiber elasticity and capillary force. With the evaporation of solvent, the drop elongated and spread spontaneously between the fibers, drawing them together to form a liquid column between the coalesced fibers. Intriguingly, further solvent evaporation allowed the long liquid column to shrink and accumulate again at the free end of the deflected fibers. In this case, the Fc-FF molecules were concentrated within the drops at the free end due to capillary flow. As a result, the free ends of these two fibers adhered to each other after the solvents were fully evaporated, and a "V" shaped geometry was formed. Figure 1b schematically illustrates the wetting and drying processes (also shown in Video S1, Supporting Information). In this process, the fiber arrays served as a "pump" to transport the liquid drops from the clamped ends to the free ends. It is reasonable to assume that similar wetting and drying behavior could occur for Fc-FF solutions on arrays of other small-diameter fibers, such as FF microtubes, allowing for the fabrication of hierarchically complex micro or nanostructures.

Therefore, we designed a sequential, combinatorial co-assembly system composed of FF and Fc-FF peptides in which we applied the capillary forces underlying wetting and drying phenomena to control the formation of hierarchical structures.

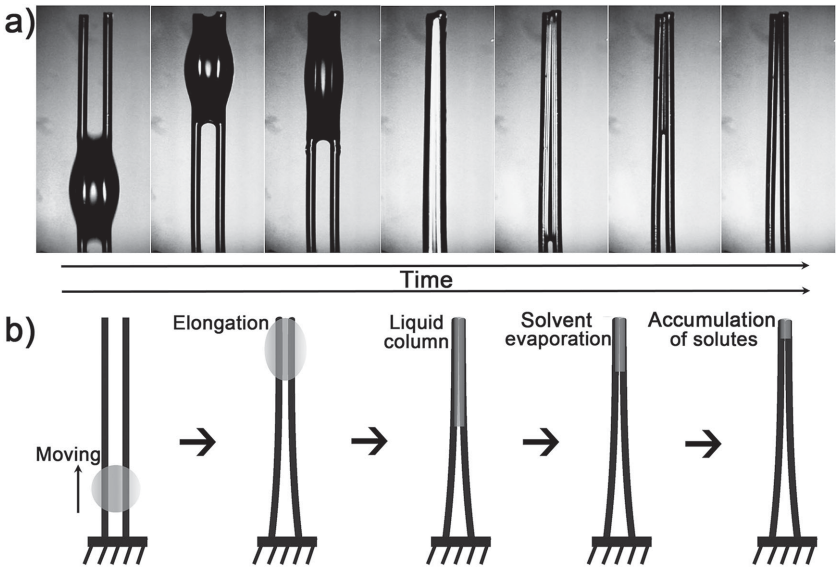

Figure 1. Wetting and drying of Fc-FF drops on arrays of two parallel fibers. a) A series of microscopy images showing the wetting and drying of 1 μL of solution (20% H_2O/80% HFIP) containing Fc-FF (5 mg mL^{-1}) on two parallel fibers (150 μm apart) that are clamped at one end and free to move at the other end. b) Schematic illustration of the wetting and drying process.

In this system, two key issues needed to be addressed at different stages of the co-assembly process. First, uniform FF microtubes must be synthesized with the desired flexibility; flexibility is closely related to fiber geometry (i.e., the diameter and wall thickness of the FF microtubes, crucial parameters affecting the wetting and drying of drops on parallel fibers).[22–24] Second, the assembly order of the FF and Fc-FF peptides must be controllable under the same conditions. The FF microtubes were initially required to generate a suitable fiber geometry. This geometry then induced capillary forces during the wetting and drying of the Fc-FF solution and led to the self-assembly of Fc-FF on the microtube arrays. In particular, previous studies have demonstrated the formation of FF microtubes via a hierarchical self-assembly process where FF molecules first self-assembled into nanotubes, and then these nanotubes further packed together to form hexagonal microtubes.[42] In this work, the FF microtubes were synthesized by first dissolving FF in ultrapure water at 65 °C, then annealing this solution at room temperature for one day. However, it is difficult to use this method to precisely control the structures (e.g., diameter or wall thickness) of the FF microtubes. The resulting FF microtubes were heterogeneous, and the sample contained tubes with a large distribution of diameters. Moreover, many solid FF microrods or nanowires were also formed in this process. To address this issue, we developed a new strategy to control the self-assembly of FF peptides into homogeneous microtubes with precisely tailored architectures.

2.2. Self-Assembly of Homogeneous, Hexagonal FF Microtubes with Precisely Tailored Diameters and Wall Thickness

The crystallization process is ubiquitous in chemistry and chemical engineering. To obtain homogenous crystals of a desired structure, one can control the degree of supersaturation, which significantly influences the size, shape, and crystal system of the products.[44–46] Inspired by this concept, we designed a novel strategy that can be used to direct the hierarchical self-assembly of FF into microtubes by controlling the degree of supersaturation. As illustrated in **Figure 2**a,b, the lyophilized FF powder was dissolved in 1, 1, 1, 3, 3, 3-hexafluoro-2-propanol (HFIP) and then diluted in methanol (CH_3OH) to create a supersaturated FF solution. Then, a small amount of water was added to trigger the self-assembly of the FF peptides into homogeneous hexagonal microtubes. Here, we defined two experimental parameters: R_v (the volume ratio of methanol to HFIP) and R_m (the mole ratio of H_2O to FF). The solubility of FF in these solvents is HFIP > methanol > water, so we can control the degree of supersaturation of the FF solutions at different R_v and R_m values. The formation of hexagonal microtubes is highly dependent on the hydrogen bonding between FF ($-NH_3^+$ groups) and H_2O molecules. By controlling the water content in the FF solution (R_m values), we were able to precisely adjust the strength of the hydrogen bonding interactions as well as the other weak interactions (e.g., hydrophobic interactions) during the hierarchical self-assembly process. As shown in Figure S2, Supporting Information, homogeneous FF microtubes with an average diameter of ≈6 μm were formed at R_v and R_m values of 0.625 and 25, respectively. We further investigated the change in diameter (D) of the FF microtubes by altering the R_v values (for R_m = 40). As shown in Figure 2c,e and Figure S3, Supporting Information, the average diameter of the FF microtubes decreased gradually from 9 to 1.2 μm as the R_v value increased from 0.5 to 1.5. Surprisingly, when the R_v value was held constant at 0.625 and the R_m value was increased from 25 to 120, a change in the average diameter of the FF microtubes was not observed (the average diameter remained constant at ≈6 μm); however, the wall-thickness (W) of the microtubes linearly increased from ≈70 to ≈950 nm (Figure 2d,f).

The effect of R_m with a value larger than 120 on the wall thickness of FF microtubes was also investigated. As shown in Figure S4a,b, Supporting Information, rigid FF microtubes with a wall thickness of ≈2 μm was formed at R_m = 200. The wall thickness is much larger than that at a lower R_m value, as demonstrated in Figure 2f. Intriguingly, further increase of R_m value to 300 led to the formation of FF microrods, as shown in Figure S4c,d, Supporting Information. These results confirm that the structural parameters, D and W, of the FF microtubes could be precisely adjusted by controlling the R_v and R_m values, respectively. In addition, the high-magnification scanning electron microscopy (SEM) images and the polarized optical microscopy graphs showed that the microtubes were composed of parallel-packed FF nanotubes

www.MaterialsViews.com

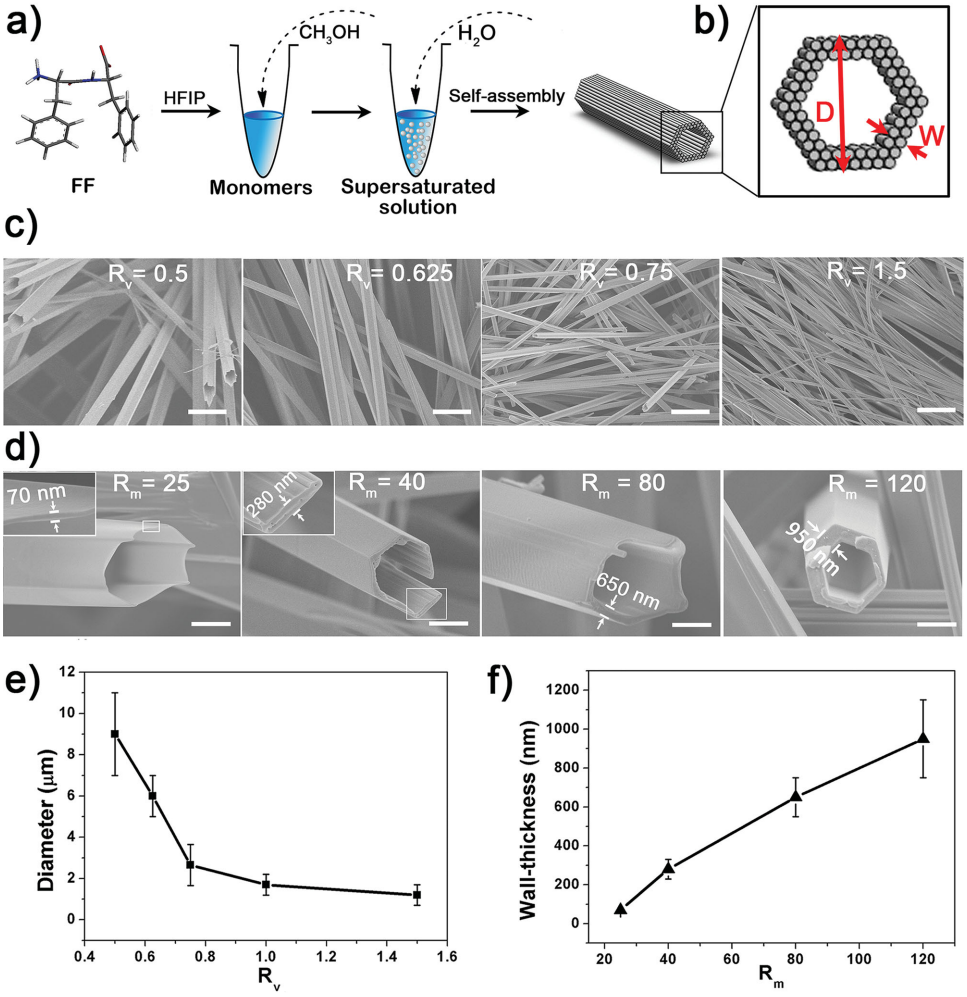

Figure 2. Self-assembly of homogeneous hexagonal FF microtubes with precisely tailored diameters and wall thickness. a,b) Schematic illustration for the hierarchical self-assembly of FF into hexagonal microtubes with tailored diameters (D) and wall thickness (W). c) SEM images of FF microtubes prepared using different R_v values (the R_m value was held constant at 40). The scale bar is 20 μm for all images. d) SEM images of FF microtubes prepared using different R_m values (the R_v value was held constant at 0.625).The scale bar is 3 μm for all images. e) The change in the average diameter of FF microtubes with increasing R_v values. f) The change in the average wall thickness of the FF microtubes with increasing R_m values.

(Figure S5, Supporting Information), indicating the existence of a hierarchical assembly mechanism similar to that previously demonstrated by Yan et al.[42] It is worth noting that the FF microtubes formed at R_m = 8 exhibited different IR adsorption properties (Figure S6, Supporting Information) and X-ray diffraction (XRD) patterns (Figure S7, Supporting Information) from those microtubes formed using R_m values of 25 and 85, respectively, indicating the important role that H_2O content plays in directing FF self-assembly likely via hydrogen bonding and hydrophobic interactions.

In this work, the initial concentration of FF in the HFIP/CH_3OH solvent ranged from 40 to 66.7 mg mL^{-1}; these concentrations are much higher than those used in previous studies.[4,42] In these cases, the average distance between individual FF molecules is very short. The solvent volume assigned to an individual FF molecule (V_i) is calculated as 7.772 nm^3 following the Equation (1)

$$V_i = \frac{M}{cN_A} \quad (1)$$

where M and c are the molecular weight and mass concentration of FF, respectively, and N_A is the Avogadro's number. When we take into account the volume of an individual FF molecule, the distance between two FF molecules is calculated to be less than 1 nm, approaching the distance required for the formation of non-covalent interactions. As a result, when H_2O molecules are introduced, networks of peptide–peptide and peptide–water hydrogen bonds are formed immediately, triggering the rapid self-assembly of FF molecules into hexagonal FF microtubes. Due to the high degree of supersaturation derived from the high concentration of FF in the HFIP/CH_3OH solvents, large quantities of crystal seeds are formed in the self-assembly process, leading to the growth of homogeneous FF microtubes with tailored diameters. In particular, only a small amount of H_2O (e.g., 0.23 mL of H_2O/100 mg of FF, R_m = 40) was required to trigger and direct the self-assembly of FF. In this case, we are able to precisely control the hydrogen bonding and hydrophobic interactions in the hierarchical self-assembly process and produce hexagonal FF microtubes with tailored diameters and wall

thickness. This method provides precise control over the uniformity, diameter, and wall thickness of the resulting FF microtubes. It is essential to be able to control such properties if such materials are to be used in practical applications. This method is thus deserving of further investigation.

2.3. Distinct Self-Assembly Behavior of FF and Fc-FF in HFIP/CH_3OH/H_2O Solutions with Different Water Contents

The distinct self-assembly behavior of FF and Fc-FF molecules in HFIP/CH_3OH/H_2O solvents is another issue that must be considered when designing the co-assembly system. Water is both a good hydrogen bond donor and acceptor, and it plays a role in the generation of hydrophobic interactions. Thus, the water content (C_w) is expected to greatly influence the self-assembly behavior of these two aromatic dipeptides. We investigated the assembly behavior of FF in HFIP/CH_3OH/H_2O solvents ($R_v = 0.625$) with water contents ranging from 0 to 33% (v/v) (R_m ranging from 0 to 120) and observed that FF microtubes slowly formed when the water content was approximately 2.76% (R_m = 8). However, the XRD pattern of the FF microtubes was not identical to that typically observed for single-crystal structures (Figure S7, black curve, Supporting Information), likely because the water molecules did not sufficiently form hydrogen bonds with the FF molecules. By increasing the water content to 8.15% (R_m = 25), the self-assembly rate significantly increased, and the formation of FF microtubes (D = 6 μm, W = 70 nm) was visually observed immediately when water was added (**Figure 3**, black curve). As mentioned above, a further increase in water content up to 33% (R_m = 120) thickened the walls of the FF microtubes (the diameters remained constant at 6 μm) (Figure 2d). The self-assembly behavior of Fc-FF was also investigated using the same procedure. As expected, well-defined assemblies were not observed when the water content was lower than 50%; however, when the water content was increased above 50%, Fc-FF self-assembled into uniform nanospheres likely due to the presence of enhanced hydrophobic interactions (Figure 3, red curve). With a further increase in water content (up to 75%), a structural transition from nanospheres to nanofibers was observed via transmission electron microscopy (TEM) (Figure 3, inset images). Intriguingly, rectangular nanotubes were formed when the water content was increased to 90%. Fourier transform infrared (FTIR) spectra indicated that the Fc-FF molecules in the nanotubes were stacked in a β-sheet arrangement (Figure S8a, Supporting Information). Moreover, small-angle X-ray diffraction (SAXD) and SEM results revealed that the rectangular nanotubes were composed of Fc-FF nanofibers that were packed in a parallel fashion and had an average diameter of ≈15 nm (Figure S8b–d, Supporting Information). The distinct self-assembly behavior of FF and Fc-FF allowed us to design and control their hierarchical co-assembly for the preparation of highly complex microstructures.

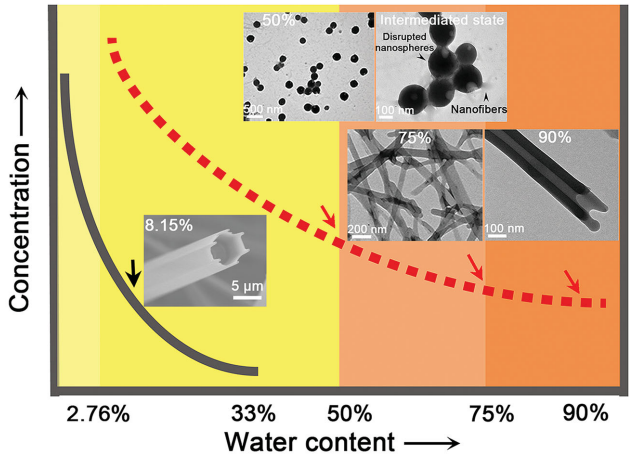

Figure 3. Self-assembly behavior of FF (black curve) and Fc-FF (red curve) in HFIP/CH_3OH/H_2O solvents for different water contents. The value of R_v was kept constant at 0.625. For FF molecules, water contents of 2.76% and 33% (v/v) correspond to R_m values of 8 and 120, respectively.

2.4. Hierarchical Co-Assembly of FF and Fc-FF into Dandelion-Like Peptide Microstructures

Our abilities to both prepare homogeneous FF microtubes with tailored diameters and wall thickness and understand the distinct assembly behavior of FF and Fc-FF motivated our efforts to program the formation of FF/Fc-FF hybrid complex structures by applying capillary forces in the wetting and drying process. FF and Fc-FF were initially dissolved in HFIP/CH_3OH solvents ($R_v = 0.625$) at final concentrations of 61.54 mg mL^{-1} and 3.08 mg mL^{-1}, respectively. Subsequently, a certain amount of water (8.15%, $R_m = 25$) was added to the resulting mixture. Upon the addition of water, FF instantly self-assembled into microtubes (observable with the naked eye), and gel-like microtube networks containing yellow Fc-FF solution formed due to the capillary force (Figure S9a, Supporting Information). The wetted FF microtube networks were then placed on glass coverslips, and solvent evaporation was allowed to occur at a relative humidity of 30% at 295 K. After drying, yellow aggregates, indicative of the self-assembly of Fc-FF molecules, were clearly observed on the surface (Figure S9b, Supporting Information). The formation of yellow aggregates at the edges of the networks was attributed to the "coffee ring" effect that is usually observed during the drying of liquid suspensions.[20]

Scanning electron microscopy was employed to characterize the resulting samples. As shown in **Figure 4**, a novel dandelion-like peptide microstructure was observed; the FF microtubes served as the "scapes" and the Fc-FF nanofibers served as the "flowers." Specifically, high-magnification SEM images (Figure 4c) revealed that the "dandelion scapes" were well-organized arrays composed of several microtubes, while the "dandelion flowers" were vertically aligned nanofibers that were formed at the ends of the microtube arrays. The distribution of tube numbers in the scape was further evaluated by SEM analysis. As shown in Figure S10, Supporting Information, the number of FF microtubes ranges from 2 to 7 and it has a maximum value of 5. The dandelion-like peptide microstructures around the edges of the array was also characterized by SEM to observe the morphology of

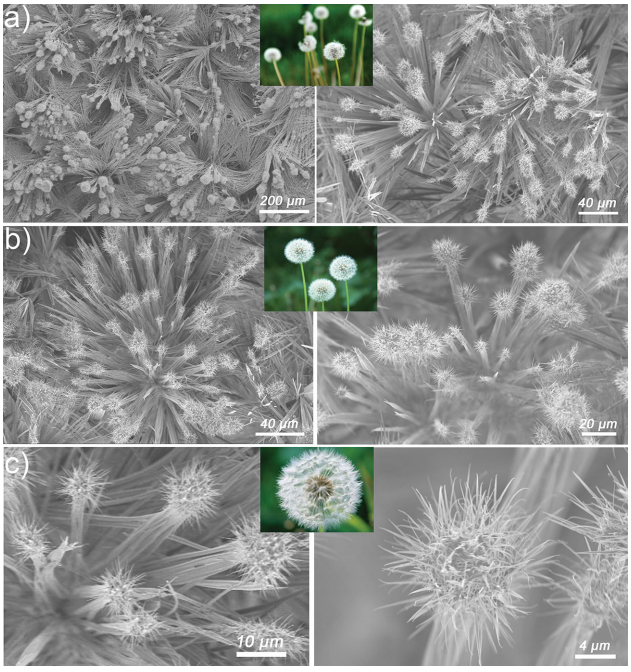

Figure 4. Scanning electron microscopy (SEM) images of the dandelion-like peptide microstructures formed via the capillary force-driven hierarchical co-assembly of FF and Fc-FF ($R_v = 0.625$, $R_m = 25$).

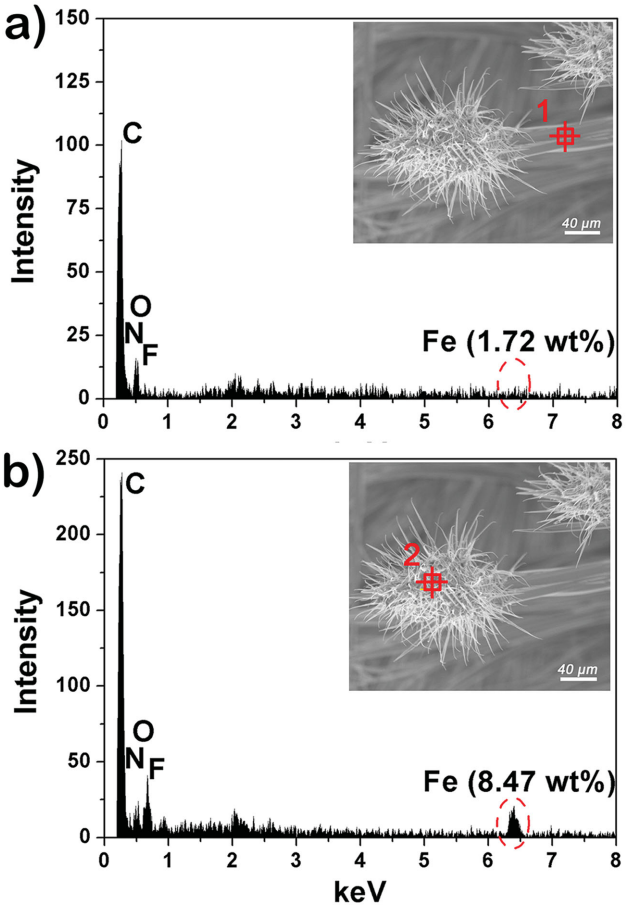

Figure 5. Micro-area elemental analysis of dandelion-like peptide microstructures by energy dispersive X-ray (EDX) spectroscopy. a) EDX spectrum and iron content of the microtube arrays that are labeled in the inset. b) EDX spectrum and iron content of the nanofibers that are labeled in the inset.

Fc-FF nanofibers. As shown in Figure S11a, Supporting Information, the density of Fc-FF "flowers" is higher around the edges because of the coffee ring effect. In addition, the slightly longer Fc-FF nanofibers were also observed around the edges (Figure S11b, Supporting Information) compared to that localized inward (Figure 4a, right). **Figure 5** shows the micro-area elemental analysis of the dandelion-like peptide microstructures obtained using energy dispersive X-ray spectroscopy (EDX). As expected, the EDX spectra indicate iron contents of 1.72 wt% and 8.47 wt% in the microtube arrays and nanofibers, respectively. The iron content of the nanofibers was close to the theoretical iron content (10.69 wt %) of the Fc-FF molecules, indicating that the self-assembled nanofibers and microtubes predominantly consisted of Fc-FF and FF molecules, respectively. These results are also consistent with those demonstrated in the single self-assembly systems (Figure 3).

We further investigated the influence of R_v and R_m values on the formation of dandelion-like peptide microstructures. As shown in Figures S12 and S13, Supporting Information, the dandelion-like microstructures were formed at $R_v = 0.625$ and $R_m = 25$–80. Particularly, the R_v values have a significant effect on the formation of such microstructures. For instance, at $R_v = 0.75$ and 1.5, the FF microtubes were horizontally arranged and no dandelion-like microstructures were observed (Figure S12c,d, Supporting Information). As for the R_m values, the results show that the dandelion-like microstructures were formed over a large range of R_m values from 25 to 80 at $R_v = 0.625$ (Figure S13a–c, Supporting Information). In these cases, the wall thickness of FF microtubes was in the range of 70 to 700 nm (Figure 2f). However, further increase the R_m to 120, no dandelion-like microstructures was observed (Figure S13d, Supporting Information), possibly due to the rigid structure derived from a large wall thickness (950 nm, Figure 2f).

Figure 6 illustrates the detailed capillary force-driven, hierarchical co-assembly process of FF and Fc-FF. Specifically, FF and Fc-FF moieties were dissolved in HFIP/CH_3OH solvents in their monomeric states, and the FF molecules were supersaturated (Figure 6a). When a small amount of H_2O was added, the FF molecules quickly self-assembled into homogeneous FF microtubes. Here, the Fc-FF molecules were still in the monomeric state owing to their low sensitivity to water (Figure 3). The assembled FF microtubes created a gel-like three-dimensional (3D) network that held a large amount of solvent and Fc-FF molecules due to capillary forces (Figure 6b). Similar behavior is seen with supramolecular hydrogels,[47,48] although the microtube network is not a soft gel because of the rigidity of the FF microtubes. The solvent at the surface of the microtube network evaporates faster than that inside the network, generating a sustainable capillary force along the direction of the microtubes that drives the flow of Fc-FF solution toward the upper surface. This flow leads to the formation of "V" shaped microtube arrays (similar to those seen in the case of the two parallel fibers, Figure 1) and the accumulation of Fc-FF molecules at

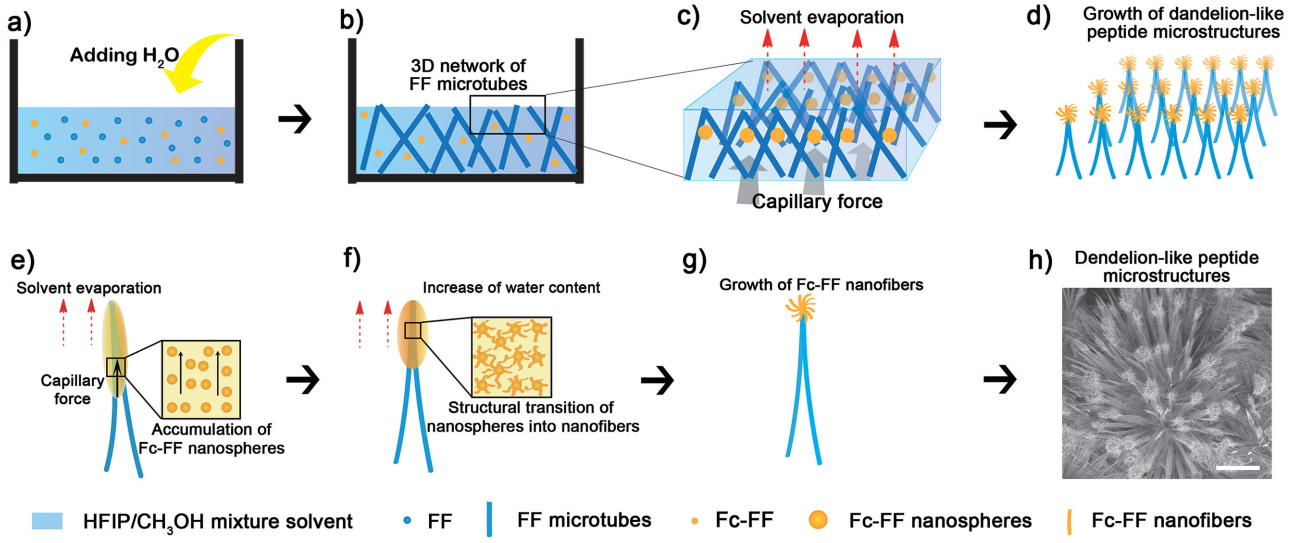

Figure 6. Schematic illustration of the capillary force-driven, hierarchical co-assembly of FF and Fc-FF peptides into dandelion-like microstructures via sequential, combinatorial assembly. a) Dissolution of FF and Fc-FF in HFIP/CH_3OH solvents. b) Formation of FF microtubes after the addition of a small amount of H_2O. The water content at this stage is relatively low, and Fc-FF molecules were still dispersed in the solvent mixture. c) Evaporation of solvents from the 3D FF microtube network. The capillary force could drive the accumulation of Fc-FF drops at the ends of the FF microtube arrays. d) Growth of dandelion-like peptide microstructures due to the self-assembly of Fc-FF at the ends of the FF microtube arrays. To clearly illustrate the co-assembly mechanism, we used two FF microtubes as the scape model. e) Schematic representation of the wetting and drying of a Fc-FF drop on two parallel FF microtubes. With the evaporation of solvents, Fc-FF molecules self-assemble into nanospheres and accumulate at the cross-points of the coalesced FF microtube arrays due to capillary forces. f) Structural transition of Fc-FF nanospheres into nanofibers with further solvent evaporation. g,h) Formation of dandelion-like peptide microstructures with FF microtubes as the scapes and Fc-FF nanofibers as the dandelion-like flower heads.

the ends of the arrays (Figure 6c). Moreover, in this process, the water content in the solution increases gradually because HFIP and methanol evaporate faster than water. As a result, Fc-FF molecules self-assemble into semi-stable nanospheres at the cross-points of the microtube arrays (Figure 6e). As water content increases further, the accumulated Fc-FF nanospheres undergo a structural transition into nanofibers (Figure 6f). Meanwhile, the capillary forces induced by the evaporation of the solvent could direct the growth of Fc-FF nanofibers along the long axes perpendicular to the periphery of the liquid drops, forming free-standing Fc-FF nanofibers (Figure 6g). A similar phenomenon also occurs as liquid drops evaporate on surfaces (known as the "coffee ring" effect).[20] This capillary force-driven, hierarchical co-assembly of FF and Fc-FF molecules leads to the formation of highly elegant and complex dandelion-like peptide microstructures (Figure 6d,h).

3. Discussion

For this work, the inspiration to program such complex peptide microstructures arose from a very simple physical phenomenon – the wetting and drying of flexible fiber arrays. Despite their ubiquity in both natural and engineered systems, comprehensive and visual studies of such processes were not reported until recently.[22–24] Based on these recent findings, we deposited a tiny drop of Fc-FF solution on a pair of parallel fibers and observed that Fc-FF solutes accumulate at the free ends of these fibers due to capillary forces. As mentioned before, the free ends of the fibers adhere to each other after the complete evaporation of the solvents, leading to the formation of a V-shaped geometry (Figure 1). These results suggest a possible strategy for directing molecular self-assembly.

In capillary force-driven co-assembly processes, the fiber geometry of the system (corresponding here to the diameter and wall-thickness of the FF microtubes) is a crucial parameter that can affect the formation of dandelion-like peptide microstructures. In regard to the microtube diameter, as shown in Figure 4 and Figure S12, Supporting Information, the SEM results show that the dandelion-like microstructures were formed only when the microtube diameter was approximately 6 μm (R_v = 0.625). Since the diameter of FF microtubes is highly dependent on the R_v value, a significant shift of the diameter is achieved when the R_v value is varied from 0.5 to 0.75 (Figure 2e). The microtubes with a large (e.g., 9 μm at R_v = 0.5) and small (e.g., 1–3 μm at R_v = 0.75–1.5) diameter are too rigid or flexible and thus cannot provide a fiber geometry suitable for the generation of capillary forces that are essential for the formation of dandelion-like microstructures. As for the wall thickness, the SEM results show that the dandelion-like microstructures were formed over a large range of wall thickness from 70 to 700 nm (R_m = 25–80) (Figure S13a–c, Supporting Information), indicative of a suitable geometry for the generation of capillary forces. However, further increase the wall thickness to 950 nm at R_m = 120 leads to a rigid structure and thus no dandelion-like microstructures were observed (Figure S13d, Supporting Information).

Another apparent feature in the capillary force-driven co-assembly processes is the growth of Fc-FF nanofibers on

the ends of FF microtube array. In views of the hydrophobic interactions between FF and Fc-FF, FF microtubes may be able to nucleate growth of the Fc-FF nanofibers at appropriate water content. For the self-assembly of Fc-FF alone, as shown in Figure 3, Fc-FF nanospheres and nanofibers were formed at a critical water content (C_w) of 50% and 75%, respectively. We further investigated the effect of microtube-induced nucleation of Fc-FF on the critical water content. For this purpose, the self-assembly of Fc-FF in the presence of FF microtubes at a water content of 40% and 65%, respectively, were characterized by SEM analysis. In the experiments, FF microtubes were prepared at $R_v = 0.625$ and $R_m = 25$, filtrated for solvents removal, and then added the Fc-FF assembly media to a final concentration of 4 mg mL^{-1}. As shown in Figure S14a, Supporting Information, no Fc-FF nanospheres was observed at C_w = 40%, indicating that the microtube-induced nucleation cannot significantly reduce the critical water content for the formation of nanospheres. As expected, Fc-FF nanospheres, but no nanofibers, were observed at C_w = 65% (Figure S14b, Supporting Information). Moreover, the dandelion-like peptide microstructures formed by the co-assembly of FF/Fc-FF show that the growth of Fc-FF nanofibers occurred on the ends of FF microtubes, rather than on the outer surfaces of the tube walls, which also exhibit hydrophobic character similar to the tube ends. Therefore, we infer that the Fc-FF nanofibers grow on the ends of FF microtubes mainly due to the increased water content in that area during the evaporation process. In this process, the ends of FF microtubes may also be able to nucleate the growth of the Fc-FF nanofibers at appropriate water content. It is worth noting that the drying speed is an important parameter for the formation of such microstructures. To demonstrate this point, we investigated the formation of complex structures in a very fast drying manner. As shown in Figure S15, Supporting Information, when the mixture was vacuum-dried, no dandelion-like peptide microstructures was observed. In this case, no accumulation of Fc-FF droplets at the ends of FF microtube arrays due to the rapid evaporation of solvent. It appears that many microtubes come together into large bundles, possibly due to the self-assembly or aggregation of Fc-FF among the FF microtubes. As illustrated in Figure 6, the formation of dandelion-like peptide microstructures is a sequential, combinatorial self-assembling process, which involves the accumulation of droplets at the ends of FF microtubes array. Therefore, this process should proceed at a slow drying speed.

Additionally, the self-assembly of Fc-FF into nanospheres and the structural transition of these spheres into nanofibers occurred at higher water contents (Figure 3) are essential to the formation of such complex microstructures. A control experiment was performed using another self-assembling peptide, *N*-fluorenylmethoxycarbonyl diphenylalanine (Fmoc-FF, Figure S16a, Supporting Information).[47,48] Fmoc-FF is a well-known gelator that can self-assemble into flexible and long nanofibers in an aqueous solution. In this study, the results indicate that the Fmoc-FF gel composed of flexible nanofibers was formed when the water content is up to 40%, as shown in Figure S16b,c, Supporting Information. Therefore, when the co-assembly of FF and Fmoc-FF occurred under the same conditions, as the evaporation proceeded, a large amount of the flexible Fmoc-FF nanofibers were generated when the water content increased to 40%. It is difficult for these entangled nanofibers to move in the FF microtube arrays. Therefore, the co-assembly of FF and Fmoc-FF just led to the microtubes-nanofibers mixture, rather than dandelion-like peptide microstructures (Figure S16d, Supporting Information).

Traditional strategies employed to control supramolecular self-assembly involve the modification of molecular structure,[5,8] solvent,[33] temperature,[36] and pH,[49] among other parameters. In addition, some other strategies exist in which templates,[50] interfaces,[16,34,51] pathway control,[11] or external forces[52] play key roles in directing molecular self-assembly. However, most of these strategies have focused primarily on defining the initial conditions. The driving force to sustain a self-assembly process is determined at the beginning and will not be changed or controlled during the hierarchical assembly process. It is impossible for a single strategy to satisfy all the requirements necessary to control hierarchical self-assembly processes. Our findings demonstrate that highly complex peptide microstructures can be formed by applying control at different stages of the hierarchical co-assembly process. By controlling the degree of supersaturation, a chemical engineering concept from the field of drug crystallization, we were able to achieve homogeneous FF microtubes with arbitrarily tailorable diameters and wall thickness (Figure 2). Because FF and Fc-FF exhibited distinct self-assembly behavior depending on the water content of the system (Figure 3), we further employed the capillary forces derived from the wetting and drying process to program the assembly of dandelion-like peptide microstructures (Figure 4). We believe that the concepts and strategies proposed in this study open new avenues for controlling hierarchical co-assembly processes and achieving highly complex nano or microstructures.

Furthermore, there are several reasons why we selected FF and Fc-FF as the model components in our investigation. First, FF is a small self-assembling peptide that has important implications in the field of supramolecular self-assembly. The investigation of this peptide can be traced back ten years.[4] Studies have revealed that FF can self-assemble into various architectures with potential applications in templation,[4,35,36] drug release,[37] the creation of superhydrophobic surfaces,[38] biosensing,[39] piezoelectric devices,[40,41] and optics.[42,43] However, it is still challenging to precisely control the structure of FF assemblies, making it difficult to use FF-based peptide materials in applications. The procedure proposed herein provides a simple and feasible approach for the preparation of homogeneous FF microtubes with arbitrarily tailorable diameter and wall thickness, and this strategy is important for their use in practical applications. Second, FF and Fc-FF are two functional self-assembling peptides. The ferrocenyl moiety may endow the Fc-FF molecule with special redox,[53] optical,[54,55] and molecular recognition[56,57] properties that could be useful in many areas of nanoscience. We believe that the co-assembly of FF and Fc-FF peptides can lead to the formation of elegant dandelion-like peptide microflowers, which may have potential applications in biosensing, optics,

and the formation of superhydrophobic surfaces. These topics are worthy of further investigation.

4. Conclusions

In conclusion, we demonstrated that homogeneous FF microtubes with precisely tailored diameters and wall thickness could be synthesized by controlling the degree of supersaturation and water content. Furthermore, inspired by the wetting and drying phenomena observed with two parallel fibers, we developed a novel co-assembly system that employs FF and Fc-FF in the fabrication of dandelion-like microstructures. In this process, gel-like FF microtube networks were initially formed upon the addition of water as a triggering solvent. Afterwards, the capillary forces derived from the wetting and drying of the Fc-FF solution on the FF microtube arrays drove the flow toward the ends of the arrays, leading to the accumulation and self-assembly of Fc-FF at the crosspoints of the FF microtubes. This hierarchical, combinatorial self-assembly finally led to the formation of novel dandelion-like peptide microstructures, where the FF microtube arrays served as the scapes and the Fc-FF nanofibers served as the flower heads. The simple and ingenious strategies presented in this study offer a creative way to control the hierarchical self-assembly process and thus to build highly complex and functional nano or microstructures.

5. Experimental Section

Chemicals and Materials: Diphenylalanine peptide (FF) and Fmoc-FF were purchased from Bachem (Switzerland). Ferrocene-diphenylalanine (Fc-FF) was synthesized according to literature procedures.[8] Ferrocene carboxylic acid was purchased from J&K Scientific Ltd (China), *O*-(Benzotriazol-1-yl)-*N*, *N*, *N*′, *N*′-tetramethyluronium tetrafluoroborate (TBTU) was obtained from Alfa Aesar (China), and 1, 1, 1, 3, 3, 3-hexafluoro-2-propanol (HFIP) was purchased from Aladdin Reagent Corporation (China). All other chemicals were purchased from Tianjin Guangfu Fine Chemical Research Institute (China).

Wetting and Drying of the Fc-FF Solution on Two Parallel Glass Fibers: A drop (1 μL or 2 μL) of solvent (80% HFIP and 20% H_2O containing 5 mg mL^{-1} Fc-FF) was deposited on a pair of parallel fibers that were clamped at one end and free to move at the other end. The diameters and lengths of the glass fibers were 50 μm and 2.6 cm, respectively. The movies and images were captured using a polarized optical microscope (POM, Sunny Instruments Co., Ltd, China) equipped with an attached charge-coupled device video camera.

Fabrication of Homogeneous FF Microtubes with Tailored Diameters and Wall Thickness: The fabrication of homogenous FF microtubes was achieved by controlling the degree of supersaturation. In a typical experiment, FF powder was dissolved in HFIP at a concentration of 100 mg mL^{-1}, and this solution was then diluted in methanol to give a final concentration of 61.54 mg mL^{-1} (R_v = 0.625); in this way, a highly supersaturated FF solution was prepared. Subsequently, a small amount of water (e.g., 0.23 mL H_2O/100 mg FF, R_m = 40) was added to the FF solution, leading to the formation of a large quantity of microtubes, which could be observed with the naked eye. The effects of the volume ratio of methanol to HFIP (R_v = 0.5–1.5) and the mole ratio of H_2O to FF (R_m = 25–300) on the diameter (D) and wall thickness (W) of the FF microtubes were investigated.

Self-Assembly of Fc-FF in a HFIP/CH_3OH/H_2O Solvent Mixture: In a typical experiment, lyophilized Fc-FF powder was dissolved in a HFIP/CH_3OH mixture (R_v = 0.625) at concentrations ranging from 2.5 to 20 mg mL^{-1}. Then, the mixture was diluted with the appropriate amount of deionized water (H_2O) to give a final concentration of 2 mg mL^{-1}. The water content in the mixture could be adjusted by changing the initial Fc-FF concentration in the HFIP/CH_3OH mixture. The resulting Fc-FF solution was then incubated for 12 h at 25 °C without being disturbed.

Co-Assembly of FF and Fc-FF into Dandelion-Like Peptide Microstructures: In a typical experiment, FF and Fc-FF powders were first dissolved in a HFIP/CH_3OH solvent mixture (1.625 mL, R_v = 0.625) to a final concentration of 61.54 mg mL^{-1} and 3.08 mg mL^{-1}, respectively. Then, 0.15 mL of H_2O (8.45% v/v, R_m = 25) was added to the solution. FF microtubes were formed immediately as observed with the naked eye, producing a three-dimensional (3D) gel-like network containing yellow Fc-FF solution. Subsequently, the FF microtube networks were placed on a glass coverslip, allowing the solvent to evaporate at ambient temperature (295 K, 30% relative humidity). The formation of yellow assemblies was observed visually on the surface of the FF microtube networks as the solvent evaporated and the samples dried.

Characterization: The morphologies of the peptide assemblies were characterized using a S-4800 field emission scanning electron microscope (FESEM, Hitachi High-Technologies Co., Japan) at an acceleration voltage of 3 kV. Energy-dispersive X-ray (EDX) spectroscopy was performed using a S-4800 SEM equipped with an energy-dispersive X-ray spectrometer (Hitachi High-Technologies Co., Japan). Transmission electron microscopy (TEM) analysis was carried out using a JEOL 1200EX electron microscope operated at 80 kV. Small- and wide-angle X-ray diffraction (XRD) measurements were performed using a PANalytical/X'Pert PRO MPD system with a Cu/Kα radiation source (λ = 1.5406 Å). Fourier transform infrared (FTIR) spectroscopy was recorded on a JASCO FT/IR-660 Plus spectrophotometer. Optical microscopy imaging was performed using a polarized light microscope (Sunny Instruments Co., Ltd, China) equipped with an attached charge-coupled device video camera.

Supporting Information

Supporting Information is available from the Wiley Online Library or from the author.

Acknowledgements

Y.W. and R.H. contributed equally to this work. This work was supported by the Natural Science Foundation of China (Grant Nos. 21476165, 51173128, and 21306134), the 863 Program of China (Grant No. 2013AA102204), the Ministry of Science and Technology of China (Grant No. 2012YQ090194), the Ministry of Education

(Grant No. 20130032120029), the Beiyang Young Scholar of Tianjin University (2012), and the Program of Introducing Talents of Discipline to Universities of China (Grant No. B06006).

[1] G. M. Whitesides, B. Grzybowski, *Science* **2002**, *295*, 2418.
[2] W. L. Noorduin, A. Grinthal, L. Mahadevan, J. Aizenberg, *Science* **2013**, *340*, 832.
[3] J. Y. Zheng, Y. Yan, X. Wang, Y. S. Zhao, J. Huang, J. Yao, *J. Am. Chem. Soc.* **2012**, *134*, 2880.
[4] M. Reches, E. Gazit, *Science* **2003**, *300*, 625.
[5] J. D. Hartgerink, E. Beniash, S. I. Stupp, *Science* **2001**, *294*, 1684.
[6] L. Zhang, L. Qin, X. Wang, H. Cao, M. Liu, *Adv. Mater.* **2014**, *26*, 6959.
[7] S. Ghosh, M. Reches, E. Gazit, S. Verma, *Angew. Chem. Int. Ed.* **2007**, *119*, 2048.
[8] Y. Wang, R. Huang, W. Qi, Z. Wu, R. Su, Z. He, *Nanotechnology* **2013**, *24*, 465603.
[9] L. Adler-Abramovich, D. Aronov, P. Beker, M. Yevnin, S. Stempler, L. Buzhansky, G. Rosenman, E. Gazit, *Nat. Nanotechnol.* **2009**, *4*, 849.
[10] J. Ryu, C. B. Park, *Adv. Mater.* **2008**, *20*, 3754.
[11] S. Zhang, M. A. Greenfield, A. Mata, L. C. Palmer, R. Bitton, J. R. Mantei, C. Aparicio, M. O. de La Cruz, S. I. Stupp, *Nat. Mater.* **2010**, *9*, 594.
[12] R. L. Huang, W. Qi, L. B. Feng, R. X. Su, Z. M. He, *Soft Matter* **2011**, *7*, 6222.
[13] K. Simkiss, K. M. Wilbur, *Biomineralization*, Academic Press, New York, **1989**.
[14] S. Yuran, Y. Razvag, M. Reches, *ACS Nano* **2012**, *6*, 9559.
[15] Q. Zou, L. Zhang, X. Yan, A. Wang, G. Ma, J. Li, H. Möhwald, S. Mann, *Angew. Chem. Int. Ed.* **2014**, *126*, 2398.
[16] Y. Wang, W. Qi, R. Huang, R. Su, Z. He, *RSC Adv.* **2014**, *4*, 15340.
[17] R. Huang, S. Wu, A. Li, Z. Li, *J. Mater. Chem. A* **2014**, *2*, 1672.
[18] R. Huang, M. Wu, M. J. Goldman, Z. Li, *Biotechnol. Bioeng.* **2015**, DOI: 10.1002/bit.25536.
[19] P. Ball, *The Self-Made Tapestry: Pattern Formation in Nature*, Oxford University Press, Oxford, **2001**.
[20] R. D. Deegan, O. Bakajin, T. F. Dupont, G. Huber, S. R. Nagel, T. A. Witten, *Nature* **1997**, *389*, 827.
[21] P. Neogi, *J. Colloid Interface Sci.* **1985**, *105*, 94.
[22] C. Duprat, S. Protiere, A. Beebe, H. Stone, *Nature* **2012**, *482*, 510.
[23] S. Protiere, C. Duprat, H. Stone, *Soft Matter* **2013**, *9*, 271.
[24] C. Duprat, A. D. Bick, P. B. Warren, H. A. Stone, *Langmuir* **2013**, *29*, 7857.
[25] W. Han, Z. Lin, *Angew. Chem. Int. Ed.* **2012**, *51*, 1534.
[26] W. Han, B. Li, Z. Lin, *ACS Nano* **2013**, *7*, 6079.
[27] S. W. Hong, M. Byun, Z. Lin, *Angew. Chem. Int. Ed.* **2009**, *48*, 512.
[28] M. Byun, W. Han, B. Li, X. Xin, Z. Lin, *Angew. Chem. Int. Ed.* **2013**, *52*, 1122.
[29] B. Li, W. Han, M. Byun, L. Zhu, Q. Zou, Z. Lin, *ACS Nano* **2013**, *7*, 4326.
[30] M. De Volder, A. J. Hart, *Angew. Chem. Int. Ed.* **2013**, *52*, 2412.
[31] M. De Volder, S. H. Tawfick, S. J. Park, D. Copic, Z. Zhao, W. Lu, A. J. Hart, *Adv. Mater.* **2010**, *22*, 4384.
[32] B. Pokroy, S. H. Kang, L. Mahadevan, J. Aizenberg, *Science* **2009**, *323*, 237.
[33] R. Huang, W. Qi, R. Su, J. Zhao, Z. He, *Soft Matter* **2011**, *7*, 6418.
[34] R. Huang, R. Su, W. Qi, J. Zhao, Z. He, *Nanotechnology* **2011**, *22*, 245609.
[35] J. Ryu, C. B. Park, *Angew. Chem. Int. Ed.* **2009**, *48*, 4820.
[36] Y. Song, S. R. Challa, C. J. Medforth, Y. Qiu, R. K. Watt, D. Peña, J. E. Miller, F. van Swol, J. A. Shelnutt, *Chem. Commun.* **2004**, 1044.
[37] R. F. Silva, D. R. Araujo, E. R. Silva, R. A. Ando, W. A. Alves, *Langmuir* **2013**, *29*, 10205.
[38] J. S. Lee, J. Ryu, C. B. Park, *Soft Matter* **2009**, *5*, 2717.
[39] L. Adler-Abramovich, M. Badihi-Mossberg, E. Gazit, J. Rishpon, *Small* **2010**, *6*, 825.
[40] A. Kholkin, N. Amdursky, I. Bdikin, E. Gazit, G. Rosenman, *ACS Nano* **2010**, *4*, 610.
[41] E. Bosne, A. Heredia, S. Kopyl, D. Karpinsky, A. Pinto, A. Kholkin, *Appl. Phys. Lett.* **2013**, *102*, 073504.
[42] X. Yan, J. Li, H. Möhwald, *Adv. Mater.* **2011**, *23*, 2796.
[43] A. Handelman, S. Lavrov, A. Kudryavtsev, A. Khatchatouriants, Y. Rosenberg, E. Mishina, G. Rosenman, *Adv. Optical Mater.* **2013**, *1*, 875.
[44] J. B. Rawlings, S. M. Miller, W. R. Witkowski, *Ind. Eng. Chem. Res.* **1993**, *32*, 1275.
[45] M. Fujiwara, Z. K. Nagy, J. W. Chew, R. D. Braatz, *J. Process Control* **2005**, *15*, 493.
[46] G. X. Zhou, M. Fujiwara, X. Y. Woo, E. Rusli, H.-H. Tung, C. Starbuck, O. Davidson, Z. Ge, R. D. Braatz, *Cryst. Growth Des.* **2006**, *6*, 892.
[47] A. Mahler, M. Reches, M. Rechter, S. Cohen, E. Gazit, *Adv. Mater.* **2006**, *18*, 1365.
[48] V. Jayawarna, M. Ali, T. A. Jowitt, A. F. Miller, A. Saiani, J. E. Gough, R. V. Ulijn, *Adv. Mater.* **2006**, *18*, 611.
[49] C. Tang, A. M. Smith, R. F. Collins, R. V. Ulijn, A. Saiani, *Langmuir* **2009**, *25*, 9447.
[50] M. Reches, E. Gazit, *Nat. Nanotechnol.* **2006**, *1*, 195.
[51] R. M. Capito, H. S. Azevedo, Y. S. Velichko, A. Mata, S. I. Stupp, *Science* **2008**, *319*, 1812.
[52] R. A Hill, V. L. Sedman, S. Allen, P. Williams, M. Paoli, L. Adler-Abramovich, E. Gazit, L. Eaves, S. J. Tendler, *Adv. Mater.* **2007**, *19*, 4474.
[53] N. C. Foulds, C. R. Lowe, *Anal. Chem.* **1988**, *60*, 2473.
[54] M. L. Green, S. R. Marder, M. E. Thompson, J. A. Bandy, D. Bloor, P. Kolinsky, R. Jones, *Nature* **1987**, *330*, 360.
[55] V. Alain, A. Fort, M. Barzoukas, C.-T. Chen, M. Blanchard-Desce, S. R. Marderm, J. W. Perryr, *Inorg. Chim. Acta* **1996**, *242*, 43.
[56] A. E. Kaifer, *Acc. Chem. Res.* **1999**, *32*, 62.
[57] J. M. Casas-Solvas, E. Ortiz-Salmerón, J. J. Giménez-Martínez, L. García-Fuentes, L. F. Capitán-Vallvey, F. Santoyo-González, A. Vargas-Berenguel, *Chem. Eur. J.* **2009**, *15*, 710.

Received: December 8, 2014
Revised: February 9, 2015
Published online: March 10, 2015